energy&fuels

Article

pubs.acs.org/EF

Catalytic Fast Pyrolysis of Pine Wood: Effect of Successive Catalyst Regeneration

Güray Yildiz,*[,†] Tom Lathouwers,[†] Hilal Ezgi Toraman,[‡] Kevin M. van Geem,[‡] Guy B. Marin,[‡] Frederik Ronsse,[†] Ruben van Duren,[§] Sascha R. A. Kersten,[∥] and Wolter Prins[†]

[†]Department of Biosystems Engineering, Ghent University, Coupure Links 653, B-9000, Ghent, Belgium

[‡]Laboratory for Chemical Technology (LCT), Ghent University, Technologiepark 918, B-9052 Ghent, Belgium

[§]Albemarle Catalysts Company BV, Nieuwendammerkade 1-3, P.O. Box 37650, 1030 BE Amsterdam, The Netherlands

[∥]Sustainable Process Technology Group, Faculty of Science and Technology, University of Twente, Postbus 217, 7500AE Enschede, The Netherlands

Supporting Information

ABSTRACT: The main product of biomass fast pyrolysis is a liquid mixture of numerous organic molecules with water that is usually called pyrolysis oil or bio-oil. The research discussed in this paper was meant (1) to validate a new, semicontinuously operated pyrolysis setup and (2) to investigate the effect of a repeatedly regenerated ZSM-5-based catalyst (eight reaction/regeneration cycles in total) on the yields and compositions of the pyrolysis products in relation to the applied process conditions and on the catalyst itself. The reliability of the setup has been proven by multiple repetition of noncatalytic and catalytic (in situ) pyrolysis experiments for pine wood at 500 °C under identical conditions. As a result, the mass balance closures for all experiments varied from 92 to 99 wt %, while the scatter in measured data was always less than 5%. Changes in the performance of the repeatedly regenerated catalyst have been observed via detailed analysis of the bio-oil (GC × GC-FID and GC × GC-TOF-MS, Karl Fischer), the noncondensable gases (micro-GC), and the carbonaceous solids (elemental analyzer, BET surface area). Along the reaction/regeneration sequence, the yield of organics increased, while water, carbonaceous solids, and noncondensable gases decreased. Trends in pyrolysis product yields converging to that of noncatalytic levels were observed, which revealed that the influence of the catalyst slowly declined. The main observation was that the catalyst partially loses its activity in terms of the product distribution along the reaction/regeneration sequence, while retaining sufficient activity in producing the target chemical compounds.

1. INTRODUCTION

Increasing prices, shortage, storage, safety, and transport of the fossil fuel feedstocks have led to an increasing interest in the use of renewable lignocellulosic biomass resources. As an abundant and fast growing organic carbon and hydrogen source, biomass is the only alternative to fossil fuels from which petroleum-like products can be produced.[1] Fast pyrolysis, the rapid thermal decomposition of matter in the absence of oxygen followed by direct condensation of vapors, is an emerging and cost-effective thermochemical method to convert solid biomass into a liquid.[2]

In the past, quite some attention was paid to optimizing the conditions of the pyrolysis process for producing a uniform, ash-free liquid intermediate (bio-oil) with significantly increased volumetric energy density in comparison to the solid biomass.[3] Although the applications are still not all fully developed, bio-oil could in principle be used as a fuel for gasifiers, boilers, engines, and turbines or serve as a biobased feed material in the existing petroleum refinery. The latter would require a certain degree of upgrading including the (partial) removal of oxygen and cracking of the oligomers present in bio-oil. In fast pyrolysis, the maximal bio-oil yield and its quality are determined by process variables such as feedstock type, pyrolysis temperature, heating rate of the biomass particles, and the residence times of both the biomass particles and the produced vapors. A careful design of the pyrolysis reactor and the vapor condensation system is crucial in that respect.[4,5]

The adverse properties of bio-oil include its water content (15−30%), the high oxygen content (35−40 wt %), its acidity (pH of 2−3), the low heating value if compared to fossil fuels (LHV of approximately 17 MJ/kg), poor volatility, and the presence of small particulates. Its immiscibility with hydrocarbon fuels and its instability under storage and heating conditions further obstruct its direct use in almost any application.[6−8]

Before bio-oil can be used in replacing petroleum fuels its quality needs to be improved by physical stabilization (fractionation, filtration, solvent addition) and/or by (thermo-) chemical upgrading.[9] Thermochemical upgrading includes either the use of heterogeneous catalysts in the pyrolysis process itself (catalytic fast pyrolysis; CFP) or secondary treatment of the liquid product in a catalytic process called hydro-deoxygenation. For further information regarding catalytic hydro-deoxygenation of bio-oil, the reader is referred to the recent publication by Dickerson and Soria.[10] Catalytic pyrolysis induces reactions that cause a change in oxygen functionalities, increase the calorific value, and improve the stability of the

Received: March 21, 2014
Revised: June 3, 2014
Published: June 3, 2014

   dx.doi.org/10.1021/ef500636c | Energy Fuels 2014, 28, 4560−4572

bio-oil. The products are more similar in chemical composition to current gasoline and diesel fuels than the conventional bio-oil.[11,12] However, low product yields and high coke formation are the major obstacles.[11,13]

In a catalytic pyrolysis process, the heat transfer material, generally assumed inert in conventional fast pyrolysis, is (partially) replaced by a solid catalyst. The presence of the catalyst lowers the temperature of the pyrolysis process[14] and favors oxygen removal via decarbonylation (CO rejection), decarboxylation (CO_2 rejection), and dehydration (H_2 consumption to form H_2O) reactions. Optimal operating temperature of the catalyst, the type of the biomass feedstock, the catalyst-to-feed ratio, and the type of the catalyst (including pore size, acidity, nature of active sites, and the presence of metals) all influence the ultimate composition of the produced bio-oils. Thus, the selection of an appropriate catalyst is crucial for the formation of higher value compounds (phenolics, alkanes, monoaromatic hydrocarbons, etc.) from the undesirable compounds (acids, sugars, polyaromatic hydrocarbons, etc.).[9,15] Lifetime activity at various temperatures and other process conditions, deoxygenation performance, and the capability to suppress the formation of coke are important issues in the catalyst selection process. Zeolites, and particularly ZSM-5, were shown to be effective in the conversion of biomass to reasonable yield of aromatics[16] and in the selective deoxygenation of pyrolytic vapors thereby increasing the C/O ratio.[17,18] The use of zeolite cracking catalysts also leads to smaller molecules being formed, due to cracking and rearrangement of the high molecular weight molecules present in the primary pyrolysis vapors.[19,20]

One of the problems of catalytic pyrolysis, hardly discussed in the literature, is the rate and extent of deactivation of the catalyst. Deactivation implies the physical, chemical, thermal, and mechanical degradation of the catalyst leading to a reduced activity and selectivity.[21,22] Various mechanisms causing catalyst deactivation are known, such as (1) fouling, the physical adsorption of certain species on the catalyst surface that causes blocking of pores and active sites; (2) poisoning, the change of the surface structure due to the chemisorption of species on active sites; (3) attrition, which is the loss of catalytic material due to physical erosion, and (4) dealumination of the zeolite Si/Al framework by hydrolysis in the presence of acids and steam.[21,23] In catalytic pyrolysis of biomass, deactivation can be mainly attributed to coke deposition, which blocks the pores and poisons the active sites of zeolites.[24−26] Some degree of deactivation by deposition of contaminants (ash) originally present in the biomass cannot be excluded either.[8]

Similar to conventional FCC processes, the deactivated catalyst can be regenerated by a high temperature oxidative treatment meant to burn the coke off the catalyst and thereby restore its activity.[23,26] In the case of a biomass, however, the associated coke contains more oxygen and hydrogen than coke from fossil fuels. Regeneration of the catalysts thus yields water and CO_x, which for ZSM-5 and similar structured catalysts, leads to dealumination and loss of active (acid) sites.[27−29] A possible solution to this problem is a two-step regeneration method.[23,24] In a first low-temperature step (ca. 250 °C) most of the water will be released, while in a second step the temperature can be raised (to 400−700 °C) to burn the coke.[28−30] In this way the catalyst degradation may be limited because of the reduced exposure to an atmosphere containing steam at high temperatures.

A number of studies have addressed the topic of catalyst regeneration after their use in catalytic pyrolysis of biomass. A few of these studies deal with *multiple* regenerations and reuse in pyrolysis (see Table A.1 in the Supporting Information). Williams et al.[31] studied the deactivation and regeneration of ZSM-5 in the upgrading of wood pyrolysis vapors in a fluidized bed reactor (7.5 cm diameter × 100 cm high). They regenerated the catalyst in a furnace at 550 °C in the presence of air for 8 h and found that the regeneration decreases the catalytic activity. With the increasing number of reaction/regeneration cycles (in total five cycles were performed), less alkene gases were produced, oxygen containing compounds were converted less efficiently, and the carbon content of the final oil was reduced by the production of additional coke. In addition, regeneration caused a less efficient conversion of hydrocarbons to aromatics, which were the products of interest. After five reaction/regeneration cycles the production of monocyclic aromatics was reduced with 50 wt % compared to the use of the fresh catalyst. More recently, Aho et al. performed catalytic pyrolysis of pine wood in a 102 mm long dual-fluidized bed reactor (ex situ)[28] and a 590 mm long fluidized bed reactor made of Pyrex glass (in situ).[29,30] The zeolite catalysts were regenerated (single reaction/regeneration cycle in each studies) batchwise in an oven while two stages of constant temperature (250 and 450 °C) were applied. It was concluded that some Brønsted acid sites were lost during regeneration, but the surface area of the catalyst regained. Carlson et al.[32] and Paasikallio et al.[33] studied the stability of the catalyst during CFP. After purging their fluidized bed with N_2 to ensure pyrolytic conditions for the experiment, they replaced the N_2 with air for a single-step catalyst regeneration. In the work carried out by Carlson et al., deposited metal impurities were detected on the catalyst; however, the acid sites on the zeolite were not affected after 10 reaction/regeneration cycles. Paasikallio et al. found that a catalyst regeneration temperature of approximately 600 °C was not high enough to remove all of the coke deposits. Increasing the temperature to about 680 °C increased the effectiveness of the coke combustion but resulted in a lower post-regeneration specific surface area for the catalyst.

In this work, the catalytic fast pyrolysis of small pine wood particles has been studied by experiments in a newly designed mechanically agitated bed reactor at 500 °C containing ZSM-5-based catalyst particles mixed with sand in a weight ratio of 1:14. The intention was to examine the effect of repeated catalyst regeneration on the product yields and composition, as well as on the properties of the catalyst itself (coke deposition and BET surface area). Eight cycles of catalytic pyrolysis and subsequent catalyst regeneration were carried out in total. The performance of the catalyst was tested under realistic (harsh) conditions, such as

(1) Mechanical mixing of the catalyst/sand bed during the pyrolysis runs, which may promote attrition and crushing of the catalyst particles;
(2) Higher catalyst regeneration temperatures of up to 600 °C;
(3) Regeneration in the presence of the pyrolysis char, leading to the accumulation of biomass ash in the reactor bed material over the successive reaction/regeneration cycles.

dx.doi.org/10.1021/ef500636c | Energy Fuels 2014, 28, 4560−4572

2. EXPERIMENTAL SECTION

2.1. Materials. Pine, obtained from Bemap Houtmeel B.V., Bemmel, The Netherlands, was used as biomass feedstock in all experiments. This feedstock was sieved to obtain a fraction with particle sizes between 1 and 2 mm. The moisture and ash content were determined to be 7.52 wt % and 0.33 wt % on a "as-received" basis (a.r.), respectively. The proximate analysis data, the elemental composition and the higher heating values (in as received and dry basis) of the pine wood are listed in Table 1.

Table 1. Properties of Pine Wood

Proximate analysis (wt %)	
fixed carbon (d.b.)	14.96
volatiles (d.b.) [ASTM E872-82]	84.76
moisture (a.r.) [ASTM E871-82]	7.52
ash (d.b.) [ASTM E1755-01]	0.33
Ultimate analysis (d.b.) [wt %]	
C	47.10
H	5.90
O	46.40
N	0.04
S	0.06
Alkali metals (d.b.) [mg/kg]	
K	346.2
Na	10.1
Mg	112.8
Ca	767.0
HHV (a.r.) [MJ/kg][a]	18.29
HHV (d.b.) [MJ/kg]	19.77

[a]Calculated by using the Milne formula.[34]

Silica sand (obtained from PTB-Compaktuna, Gent, Belgium) with a mean diameter of 250 μm and a particle density of 2650 kg/m^3 (compacted bulk density = 1660 kg/m^3) was used as bed material for noncatalytic experiments and blended with the catalyst in the case of the in situ catalytic experiments.

A commercial, spray-dried heterogeneous ZSM-5-based catalyst was prepared and supplied by Albemarle Catalyst Company B.V. (Amsterdam, The Netherlands). Prior to the delivery, this catalyst was calcined in air at 500 °C for 1 h to decrease the moisture content of the catalyst to below 1 wt %.

2.2. Experimental Unit. Noncatalytic and in situ catalytic pyrolysis experiments have been carried out in a fully controlled, semicontinuously operated lab-scale setup that enabled the production of bio-oil samples (ca. 50 g/run) suitable for a full physicochemical characterization. A scheme of the unit is shown in Figure 1.

The electrically heated pyrolysis reactor vessel is built from stainless steel and has a design similar to the usual bubbling fluidized reactors. Its bed height, inner bed diameter, freeboard height, and freeboard diameter are 45, 7, 35, and 10 cm, respectively. A specially designed mixer was placed inside the reactor to ensure uniform mixing of the content of the bed. Cold model mixing and bed material discharging tests, performed prior to the experimental work, visually revealed the well-mixing of the bed contents (catalyst and sand) without any segregation. The rotation frequency of the mechanical mixer is adjustable via a rotor, and with the continuous rotation of the shaft, efficient mixing of the bed material is achieved and immediate contact of biomass particles with turbulently moving bed material is ensured.

Unlike fluidized bed reactors in which an inert gas is used to mix/fluidize the bed, the purpose of the inert gas in this setup is to remove the pyrolysis vapors from the reactor. The addition of a mechanical mixer inside the reactor allows the inert gas flow rate to be lower than the minimum fluidization velocity, thereby increasing the contact time of the pyrolysis vapors with the catalyst while minimizing the entrainment of the catalyst particles out of the reactor and preventing the segregation of partly converted char particles on top of the bed.

2.3. Pyrolysis Experiments. The pine wood (a.r.) is introduced into the reactor by a twin-screw from a sealed feed hopper. Inert gas (N_2) enters the system at three points, viz., via the feed hopper (~15%), the plenum chamber (preheated, ~80%), and the top of the pyrolysis reaction vessel (~5%). The flow rates of both streams were precisely controlled by individual mass flow controllers. A total inert gas flow rate of ca. 160 L h^{-1} was applied in all experiments. A knock out vessel is placed at the exit of the reactor to remove and collect fine particles. Pyrolysis vapors flow into a tap water cooled liquid recovery system that consists of an electrostatic precipitator (ESP, operated at 15 kV)

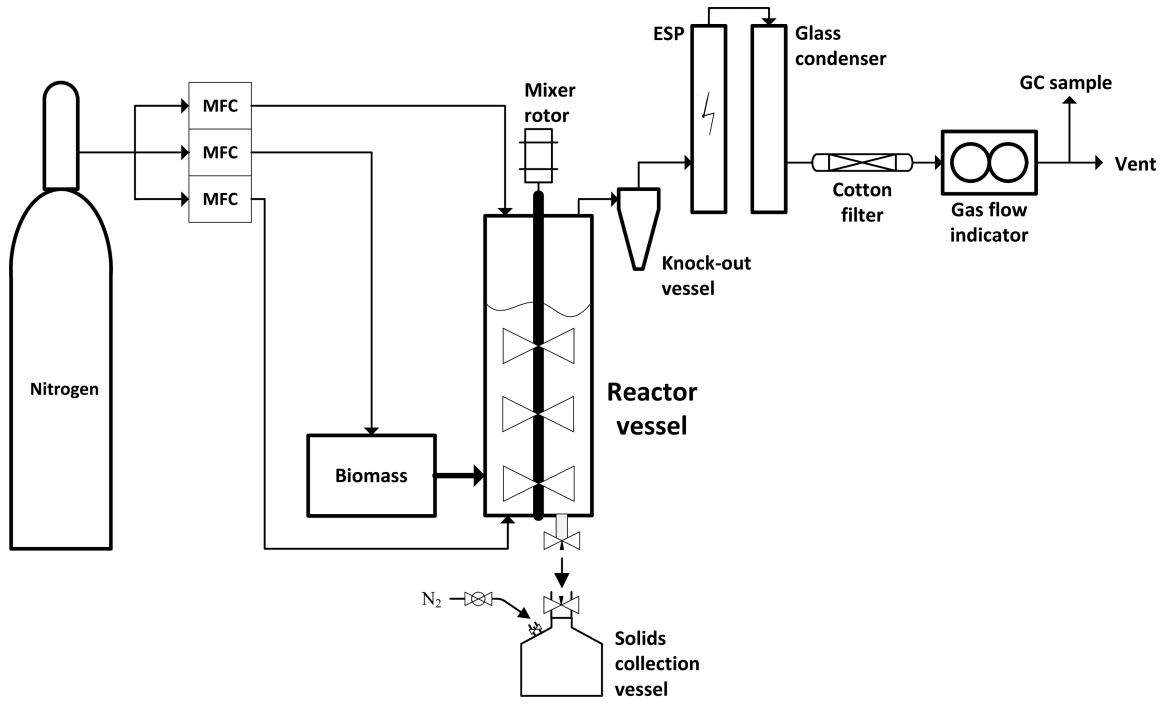

Figure 1. Scheme of the pyrolysis setup.

dx.doi.org/10.1021/ef500636c | Energy Fuels 2014, 28, 4560−4572

and a spiral condenser (glass). The noncondensable gases (NCGs) leave the system after passing through a cotton filter and a gas flow measurement. It was decided to keep the experimental run time at 60 min in order to produce sufficient bio-oil for different types of analyses as well as to reach a sufficiently high accuracy for the mass balance determination. Moreover, a relatively long experimental run time allows the biomass particles to be completely devolatilized at the reaction temperature. Approximately 100 g of pine wood is fed during every run, which could be determined by measuring the mass difference between pine in the storage hopper and in the feeding screw, before and after each experiment. For the noncatalytic experiments, 1.5 kg pure sand was used as a reactor bed material, while for the in situ catalytic experiments a catalyst−sand mixture of 1.5 kg (catalyst-to-sand mass ratio of 1:14) was used. The reason for selecting a catalyst-to-sand weight ratio of 1:14 was to maintain the weight hourly space velocity WHSV [h^{-1}] at a value of around 1 (see Table 2).

Table 2. Operating Conditions Noncatalytic and Catalytic Experiments

t_{run} [min]	60	
$T_{reactor}$ [°C]	500	
U [m/s][c]	0.012	
U/U_{mf} [−][c]	0.22	
$(U/U_{mf})_{total}$[d]	0.35	
	noncatalytic[a]	catalytic[b]
Φ_{pine} [g/h]	116.5	111.0
Φ_{N2} [L/h]	164.6	158.4
$m_{bed\ material}$ [kg]	1.5	1.5
ratio of catalyst/sand in mixture [wt/wt]		1:14
$m_{bed\ material}/m_{pine}$ [wt/wt][e]	12.9	13.5
WHSV [h^{-1}][f]		0.9
final char hold-up [vol %][e]	12.9	11.3
τ_{vapors}, in the bed material [s]	10.2	10.6
τ_{vapors}, reactor freeboard [s][g]	32.8	34.9
τ_{vapors}, total	43.0	45.5

[a]Averages of five noncatalytic experiments (NC) under identical process parameters. [b]Averages of three in situ catalytic experiments (R0) under identical process parameters. [c]On the basis of nitrogen flow only (pyrolysis vapor free stream). [d]On the basis of combined flow rate of nitrogen + pyrolysis vapors (noncatalytic case). [e]After t_{run} = 60 min. [f]WHSV (weight hourly space velocity) = mass flow rate of feed [g/h]/mass of catalyst [g]. [g]The residence time of hot vapors after they leave the bed, until they reach the condenser inlet.

2.4. Collection and Analysis of Pyrolysis Products. The products obtained from catalytic pyrolysis are divided into noncondensable gas (NCG), liquid products (organics and water), and carbonaceous material (coke/char).

The average NCG flow rate ($\Phi_{g,avg}$; L/h) was calculated by subtracting the average inert gas flow from the total gas flow. During the run, six gas samples were taken at intervals of 10 min by using a gastight syringe. The composition of noncondensable gases was determined off-line using a micro-GC (Varian 490-GC) equipped with two TCD detectors and two analytical columns. The following gaseous compounds were measured: CO, CO_2, CH_4, C_2H_4, C_2H_6, C_3H_6, C_3H_8, and H_2. The sum of C_2H_4, C_2H_6, C_3H_6, and C_3H_8 will be further referred to as C_{2+}. For detailed information concerning the NCG yield calculations, the reader is directed to our earlier publication.[35]

Prior and subsequent to each experiment, the ESP ($m_{ESP,in}$ and $m_{ESP,out}$), the glass condenser ($m_{gc,in}$ and $m_{gc,out}$) and the cotton filter ($m_{cf,in}$ and $m_{cf,out}$) (including their piping) were weighed. The mass difference should be equal to the measured amount of bio-oil produced. In order to recover the residual bio-oil fractions on the condenser walls, all related parts were rinsed with a known amount of tetrahydrofuran (THF). By using THF, a homogeneous (single-phase) liquid mixture was obtained. This mixture was then filtered over a 10 μm MN640w filter (Macherey-Nagel, Düren, Germany) and the amount of retained solids (m_{fs}) was excluded from the total amount of bio-oil. In order to prevent the solid losses and ensure a constant catalyst concentration in the bed inventory, these retained solids were included in the gross amount of bed material prior to the regeneration step. The bio-oil yield was calculated using eq 1:

$$Y_{bio\text{-}oil} = [(m_{ESP,out} - m_{ESP,in}) + (m_{gc,out} - m_{gc,in}) + (m_{cf,out} - m_{cf,in}) - m_{fs}]\frac{100\%}{m_{feed}} \quad (1)$$

The bio-oil + THF mixtures were analyzed for the H_2O content (Karl Fischer titration) and their chemical composition (GC × GC/MS-FID). For detailed characterization of bio-oils, a combination of GC × GC−FID and GC × GC−TOF−MS was used to get a high chromatographic resolution and on the other hand maximal agreement between both chromatograms.[35,36] The GC × GC setup was consisted of a Thermo Scientific TRACE GC × GC, obtained from Interscience Belgium, and has been discussed previously.[37,38] The first column was a RTX-1 PONA (50 mL × 0.25 mm I.D., 0.5 μm df) and the second column was a BPX-50 (2 mL × 0.15 mm I.D., 0.15 μm df). The oven temperature program started at −40 °C and was ramped up to 300 °C at a heating rate of 3 °C/min.[37,38] For GC × GC, the modulation period was 7 s. The mass fraction of each compound is calculated using the mass fraction of the internal standard, peak volumes obtained using the GC, and the relative (to methane) response factors of the compounds for the FID. The response factors for a large set of typical compounds that are present in bio-oils are determined experimentally from a set of well-defined calibration mixtures.[36] Response factors of compounds that were not included in the calibration mixture, and that are detected in bio-oils, were calculated using the effective carbon number approach.[39] After the identification and quantification of the compounds present in the bio-oils, the compounds were classified into eight different groups, namely, sugars, aldehydes, acids, furans, ketones, phenols, aromatics and others, according to their functional groups. More details can be found in Yildiz et al.[35] and Djokic et al.[36] Every analysis was done in triplicate, and averaged data are reported with the corresponding standard deviations.

Carbonaceous solids (CS) are the sum of char, heterogeneous coke (defined as the coke deposited on the catalyst), and system deposits. System deposits can be defined as the carbonaceous matter other than char in the case of the noncatalytic experiments, and an average value of ca. 5 wt % was obtained after having been checked a number of times. The amount of carbonaceous solids was determined by subjecting the collected solids to L.O.I. analysis, which refers to the weight loss of a sample after ignition and combustion in air which is carried out in a muffle furnace (Carbolite AAF 1100) at 600 °C for 6 h. Solids are composed of the contents of the solids collection vessel (char + bed material) and knockout vessel, and solid filtrate (washed with THF) from bio-oil filtration. The yield of carbonaceous solids was calculated using eq 2:

$$Y_{cs} = (m_{solids,i} - m_{solids,f})\frac{100\%}{m_{feed}} \quad (2)$$

The BET surface area of spent and regenerated catalysts was determined by a Gemini V surface area analyzer from Micromeritics.

The elemental composition of char samples were determined by a Thermo Scientific Flash 2000 Organic Elemental Analyzer. The elemental distribution for the pyrolysis products can be found in the Supporting Information.

The Dulong equation (eq 3) for a semiquantitatively calculation of the higher heating value's (HHV) of fuels or fuel resources, such as coal, biomass, pyrolysis oil, and biodiesel from the elemental weight composition, was used to calculate the HHV's of bio-oil samples, where C, H, and O are carbon, hydrogen, and oxygen in weight percentages, respectively:[40]

$$HHV\ (MJ{\cdot}kg^{-1}) = (337C + 1442(H - O/8))/1000 \quad (3)$$

dx.doi.org/10.1021/ef500636c | Energy Fuels 2014, 28, 4560−4572

2.5. Successive Regeneration of the Catalyst. The effect of catalyst regeneration on its activity was investigated by comparing the product yields and the compositions of bio-oil and noncondensable gases. After each experiment, the bed material (char, sand, and the spent catalyst mixture) was removed from the reactor. Small amounts of char and spent catalyst were taken for their compositional analyses, and the rest was subjected to a regeneration procedure in a muffle furnace based on the procedure proposed by Aho et al.[30] Here the temperature was increased from ambient to 250 °C with a ramp rate of 4.5 °C min^{-1} and kept isothermal at 250 °C for 40 min. Then the temperature was raised to 600 °C with a temperature increase of 5 °C min^{-1} and kept at 600 °C for 5 h. The reason to select this relatively high catalyst regeneration temperature was to maximize the removal of the heterogeneous coke deposited on the catalyst surface. The application of an even higher regeneration temperature was considered undesirable because of the risk of the surface area loss of the catalyst. The temperature was then decreased to 105 °C (instead of ambient temperature) to prevent moisture absorption. Finally the catalyst–sand mixture, regenerated in this way, was stored in the oven at 105 °C until the next experiment. Subsequently, it was fed back to the pyrolysis reactor and the experiment was repeated. In total, eight reaction/regeneration cycles were carried out.

3. RESULTS AND DISCUSSION

3.1. Mass Balance Closure and Reproducibility. The reproducibility of the setup was tested by performing a number of noncatalytic and in situ catalytic benchmark experiments under identical process conditions. These operating conditions are listed in Table 2.

The total mass balance closures calculated for the experiments varied between 92.1 wt % and 97.8 wt % for the noncatalytic and 93.1 wt % and 99.2 wt % for the in situ catalytic experiments, respectively. Small but inevitable product losses, which are inherently related to this scale of operation, are the reason that the mass balances could not be closed completely. The average product yields, on an "as received" basis, are reported in Figure 2 and were within the range of what has been

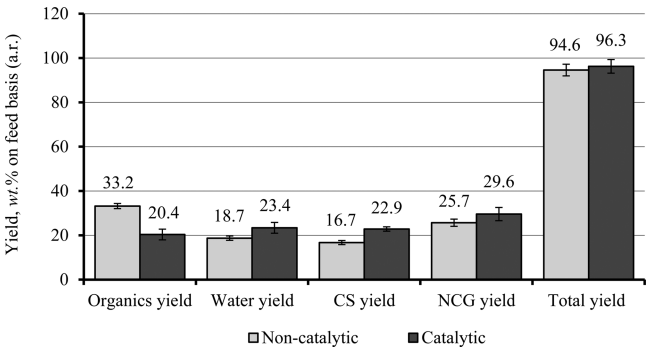

Figure 2. Yields of organics, water, carbonaceous solids (CS), noncondensable gases (NCG), and total yields obtained from five noncatalytic and three in situ catalytic fast pyrolysis with fresh catalyst experiments of pine wood at a $T_{reactor}$ of 500 °C. Standard deviations are represented in absolute %.

previously reported in the literature.[41] In this figure, the error bars represent standard deviations in absolute %'s for all experiments. Variations were mainly due to the handling, collection, and weighing of the products. The scatter in the product yields is always less than 5%, indicating reproducibility sufficient for observing trends in all similar experiments.

3.2. Effect of the Catalyst and Vapor Residence Time on Pyrolysis Product Yields. To maximize bio-oil production in biomass fast pyrolysis, vapor residence times less than 1 s are considered essential.[42] However, in the present setup, vapors reside longer in the hot zones due to the specific design of the reactor. Secondary cracking of the primary products may occur to a significant extent, which will increase the gas yields, reduce the liquid yield, and affect the bio-oil properties as well.[43] At the same time, however, these higher vapor phase residence times could promote the secondary vapor-phase cracking reactions.[33] Even though the composition of the pyrolysis oil may be dependent on the vapor residence time to a certain extent, in order to disclose the quality of our liquid product, we compared the chemical composition of a standard noncatalytic bio-oil from this study's setup with a reference bio-oil obtained from the continuous fast pyrolysis plant (with 150–200 kg/h of feed intake) of Biomass Technology Group, BTG (Enschede, The Netherlands). These results revealed that, although the produced quantity of our liquid product was lower, the chemical composition of it is similar to that produced in this continuous fast pyrolysis pilot plant (see Figure A.1 in the Supporting Information).

In the literature, catalytic fast pyrolysis mechanisms are presented, describing the reactions that take place when fast pyrolysis of biomass is carried out in the presence of zeolites.[32,44] Generally, the organic compounds formed in noncatalytic fast pyrolysis undergo an additional conversion to more desired products in the presence of a zeolite. This extra transformation often includes dehydration, decarbonylation, and decarboxylation reactions, leading to an increased production of H_2O, CO, and CO_2, of which the last two are the dominating species in the NCGs. During the catalyzed reactions, part of the intermediate compounds is also converted into coke,[45] which is mainly deposited on the catalyst. All of the carbon-containing byproducts of the catalyzed reactions (i.e., CO, CO_2, and coke) are formed at the expense of the compounds in the organic liquid fraction. These considerations are in line with our observations (Figure 2) in which the product yield distribution was considerably influenced by the presence of the catalyst. Compared to the noncatalytic case, a decrease of almost 13 wt % in the organics yield was seen in the in situ catalytic case, which is associated with an increase in water by almost 5 wt %, in carbonaceous solids by more than 6 wt %, and in noncondensable gases by around 4 wt %. The difference in yields of carbonaceous solids between noncatalytic and in situ catalytic modes can be explained by coke deposition on the catalyst since the char yields in both cases are assumed to be the same.

3.3. Effect of Successive Catalyst Regeneration on the Product Yields. The effect of successive catalyst regeneration was investigated in relation to the mass yields for organics, water, carbonaceous solids, and noncondensable gases as a function of the number of reaction/regeneration cycles (Figure 3). The values obtained from three in situ catalytic experiments with fresh catalyst were averaged and used as reference case (denoted as "R0"). The run with bed materials obtained from the first experiments after regeneration is denoted (R1), with subsequent cycles indicated by R2 to R8. In order to limit experimental errors, two experiments in parallel batches were carried out for every regeneration cycle, and the values were averaged. The experimental conditions and procedures described in sections 2.3 and 2.4 were also applied for all these tests with regenerated catalysts.

Trendlines in the graphs show clear changes for all products. In comparison with the noncatalytic experiments, a remarkable decrease in the organics yield is observed, viz. from 33.2 wt %

dx.doi.org/10.1021/ef500636c | Energy Fuels 2014, 28, 4560–4572

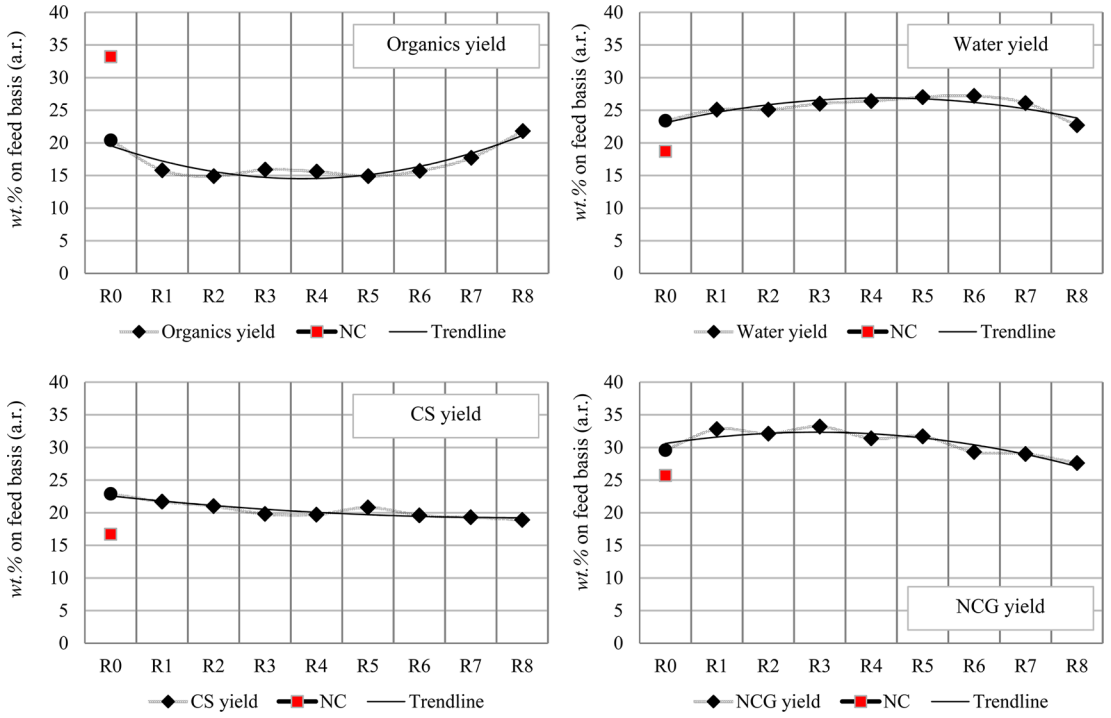

Figure 3. Influence of successive catalyst regeneration (R1 to R8, ◆) on the product yields of pine wood pyrolysis at 500 °C. Results for the noncatalytic (NC, red square) and catalytic pyrolysis with fresh catalyst (R0, ●) are included for comparison.

to 20.4 wt % for R0 (fresh catalyst) and further down to 15.8 wt % for R1 (catalyst one time regenerated). The yield of organics slightly oscillates around 15 wt % from the second to the sixth regeneration cycle and then starts to increase for the seventh and eighth regenerations to 17.7 and 21.8 wt %, respectively. This increase in liquid yields in the last reaction/regeneration cycles indicates that with the decreasing activity of the catalyst (see section 3.6) the production of a liquid similar to non-catalyzed bio-oil is favored. This results in the convergence of the yields to the noncatalytic values after a certain number of reaction/regeneration cycles. On the contrary, in the presence of fresh ZSM-5 catalyst (R0), the water yield increases from the noncatalytic level of 18.7 wt % to 23.4 wt % as discussed before in Section 3.2. The increase in water yields over the zeolites is expected as a result of more intense deoxygenation of the pyrolysis vapors.[28] When the number of catalyst regenerations is increased, the water yield becomes slightly higher until the sixth regeneration (R6) to 27.2 wt % and then starts to decrease again in the seventh and eighth regenerations to 26.1 and 22.7 wt %, respectively. These opposite trends of the organics and water yields together indicate that the deoxygenation via H_2O production passes through a maximum during successive catalyst regeneration, returning at the end (after six cycles) in the direction of the noncatalytic case.

The noncondensable gas yield for the noncatalytic experiments is 25.7 wt % and increases to 29.6 wt % after using fresh catalysts. The highest NCG yield (33.2 wt %) is found after three reaction/regeneration cycles, while after this point the yields starts to decrease gradually to a level of 27.7 wt % after the eighth regeneration, which is coming close to the value for the noncatalytic experiments.

The individual yields of char and the system deposits were assumed to be ca. 12 wt % and ca. 5 wt %, respectively for all the experiments because each experiment was carried out under identical process conditions. This has been checked a number of times. Besides, the residence time of the pine wood particles in the bed (t_{run}) was always long enough for a complete devolatilization. Hence, the differences in the yields of carbonaceous solids must represent the changes in the coke on catalyst. Figure 4 shows those changes in the coke yield as a function of the reaction/regeneration cycles. Obviously the catalyst pores are blocked by coke (and mineral) deposition, thereby limiting the access to the active surface area of the catalyst. The fresh catalyst gives a coke yield of 6.2 wt %. The coke yield then steadily decreases to a level of 2.2 wt % after the eighth regeneration. Assuming that the regeneration procedure is efficient in burning off all the coke, it is evident that coke is always formed again after each regeneration step. If the coke formation is taken as an indication of the catalyst activity, the steady decrease in coke on catalyst over the eight reaction/regeneration cycles would point at a gradually decreasing catalyst activity, which is in line with the observations regarding the product yields (Figure 3).

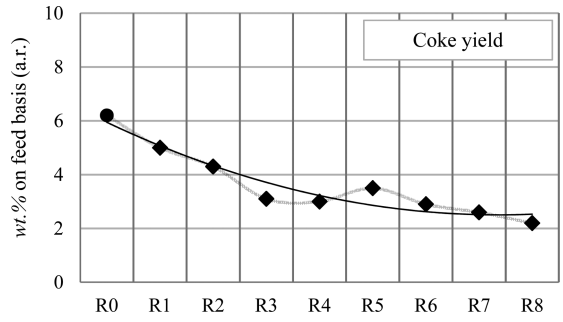

Figure 4. Changes in the coke-on-catalyst (heterogeneous coke) yield along the successive catalyst regeneration cycles. R1 to R8, ◆: experiments with pine wood at 500 °C. R0, ●: in situ catalytic fast pyrolysis with fresh catalyst.

dx.doi.org/10.1021/ef500636c | Energy Fuels 2014, 28, 4560−4572

Table 3. Yields of CO, CO_2, and H_2O in wt % on Feed Basis (a.r.), Elemental Composition of Bio-Oil (wt % in Dry Bio-Oil Basis), and the Bio-Oil Heating Value (wt % in Dry Bio-Oil Basis) Listed for All Successive Reaction/Regeneration Cycles (R0 to R8) and the Noncatalytic Case (NC)[a]

	CO	CO_2	H_2O	C	H	O	HHV (MJ kg^{-1})
NC	13.0 ± 0.8	10.0 ± 0.7	18.7 ± 1.0	60.1	5.8	34.1	22.5
R0	16.2 ± 1.7	10.1 ± 1.1	23.4 ± 2.4	70.1	5.7	24.2	27.4
R1	18.7 ± 0.8	11.4 ± 0.4	25.1 ± 0.9	75.1	5.6	19.3	29.9
R2	17.9 ± 1.2	10.7 ± 0.8	25.1 ± 3.3	77.3	5.3	17.4	30.5
R3	18.5 ± 1.2	11.3 ± 0.6	26.0 ± 2.6	76.4	5.1	18.5	29.8
R4	17.1 ± 1.5	11.1 ± 0.8	26.4 ± 4.3	75.6	5.2	19.2	29.5
R5	16.9 ± 1.6	11.7 ± 0.1	27.0 ± 2.8	77.2	4.8	18.0	29.6
R6	16.0 ± 2.2	10.6 ± 1.3	27.2 ± 1.5	76.4	4.4	19.3	28.5
R7	15.8 ± 0.5	10.0 ± 0.1	26.1 ± 0.1	74.4	5.0	20.6	28.6
R8	14.9 ± 0.3	9.7 ± 0.5	22.7 ± 0.6	66.4	5.5	28.2	25.2

[a]Experiments with pine wood at 500 °C.

3.4. Effect of Successive Catalyst Regeneration on the Deoxygenation of Pyrolysis Vapors and the Energy Density of Bio-Oils. The main goal of catalytic pyrolysis is to upgrade the highly oxygenated pyrolysis vapors by removal of the oxygen, and the cracking/rearrangement of molecules, in order to produce a liquid product rich in alkanes and aromatics.[31] The elemental distribution of the various pyrolysis products obtained after all the reaction/regeneration cycles (R1 to R8), as well as those for the noncatalytic (NC) and fresh catalyst cases (R0), were collected in Table A.2 of the Supporting Information. CO, CO_2, and H_2O are the primary products of bio-oil oxygen removal in zeolite catalytic upgrading,[45] and their yields are given in Table 3. Being the main components of the noncondensable gases, CO and CO_2 yields exhibited a trend similar to one observed for the NCG yields (see Figure 3). The noncatalytic CO yield of 13.0 wt % increased to 16.2 wt % for pyrolysis with a fresh catalyst and reached a maximum of 18.7 wt % for pyrolysis after the first regeneration, before dropping to a value of 14.9 wt % for pyrolysis after the eighth regeneration. Despite some minor differences, the CO_2 yields overall followed the same trend. In accordance with the literature, these results indeed confirmed that decarbonylation and decarboxylation, together with dehydration (Figure 3), are the main mechanisms for bio-oil deoxygenation in catalytic pyrolysis with zeolites.

Table 3 further shows that the elemental yields (wt % in dry bio-oil basis) of carbon and oxygen in bio-oil show opposite trends with respect to each other. The bio-oil carbon content passes through a maximum, while the oxygen content passed through a minimum with an increasing number of reaction/regeneration cycles. The maximum carbon content of the bio-oil was 77.3 wt % after two regeneration cycles (R2), and the lowest oxygen content was observed in R2 with a value of 17.4 wt %. The hydrogen contents in the produced bio-oils were only slightly affected by the number of catalyst regeneration cycles. On average the hydrogen content after every regeneration decreased with 10−20% in comparison to the noncatalytic case (5.8 wt %), and a minimum was observed after five to six regenerations. As an illustration of the maximal catalytic effect, one could compare the chemical formula that can be derived from the elemental composition listed in Table 3, for the noncatalytic pyrolysis (NC) with the one for catalytic pyrolysis after five regenerations (R5). It changes from $CH_{1.16}O_{0.43}$ to $CH_{0.75}O_{0.17}$, respectively. Apparently, the catalyst is effective in rejecting oxygen from the organics phase at the expense of hydrogen. The change in elemental composition can also be clearly seen in the heating value of the product oil (dry bio-oil basis), which increased from 22.5 MJ kg^{-1} for the noncatalytic case (NC) to a value of approximately 30 MJ kg^{-1} after 1−5 regenerations. Despite this remarkable increase, the energy density of the produced bio-oil was still low compared to the energy density of conventional fuels.[3] In attempt to summarize the observations collected in Table 3, one could say that the catalyst activity increases over the first two to three reaction/regeneration cycles, and then maintains it activity over a number of following cycles but finally loses part of its activity over the last two cycles R7 and R8. However, even after eight cycles, some catalyst activity was still clearly observable from the increased carbon monoxide and water production, the higher carbon and the lower oxygen contents of the product oil organics, and the corresponding rise in heating value.

Figure 5 shows the changes in CO_x yields (sum of CO and CO_2 yields), the CO/CO_2 ratio, and the changes in the yields of H_2, CH_4, and C_{2+} as a function of the increasing number of catalyst regenerations.

The trend of the CO_x yield shown in Figure 5a was similar to the one for the NCG yield shown in Figure 3. It showed the highest level of approximately 30 wt % in the beginning and then a gradual decrease to a value of 24.6 wt %, which is quite close the noncatalytic value of 22.9 wt %.

The CO/CO_2 ratio of the product gases is assumed to be a good measure to monitor the catalytic activity.[46] In Figure 5b, the CO/CO_2 ratio was shown to increase from a value of 1.3 for noncatalytic pyrolysis to 1.6 for pyrolysis in the presence of the fresh catalyst (R0). The trend was then slightly downward, viz., to a value of about 1.54 after eight cycles. Apparently, the presence of catalyst favors the decarbonylation mechanism over the decarboxylation mechanism during all the successive reaction/regeneration cycles. Remarkable was the single oscillation in CO/CO_2 between a maximum value of 1.68 and a minimum value of 1.50.

The CH_4 yields decreased from a noncatalytic value of 1.64 wt % to the value of 1.32 wt % in R0 when the catalyst was added (Figure 5c). Then, in a slightly fluctuating way, it steadily increased to the value of 1.60 wt % after eight regenerations (R8), close to the value for the noncatalytic pyrolysis. On the contrary, the C_{2+} yield (C_2H_4 was being the most abundant hydrocarbon) jumped to a peak value of 1.02 wt % in R1 and then started to decrease steadily to a value of 0.54 wt % in R8 (Figure 5d). The higher level of C_{2+} yield in catalytic pyrolysis was likely caused by secondary cracking of heavier molecules to lower molecular weight hydrocarbons.

dx.doi.org/10.1021/ef500636c | Energy Fuels 2014, 28, 4560−4572

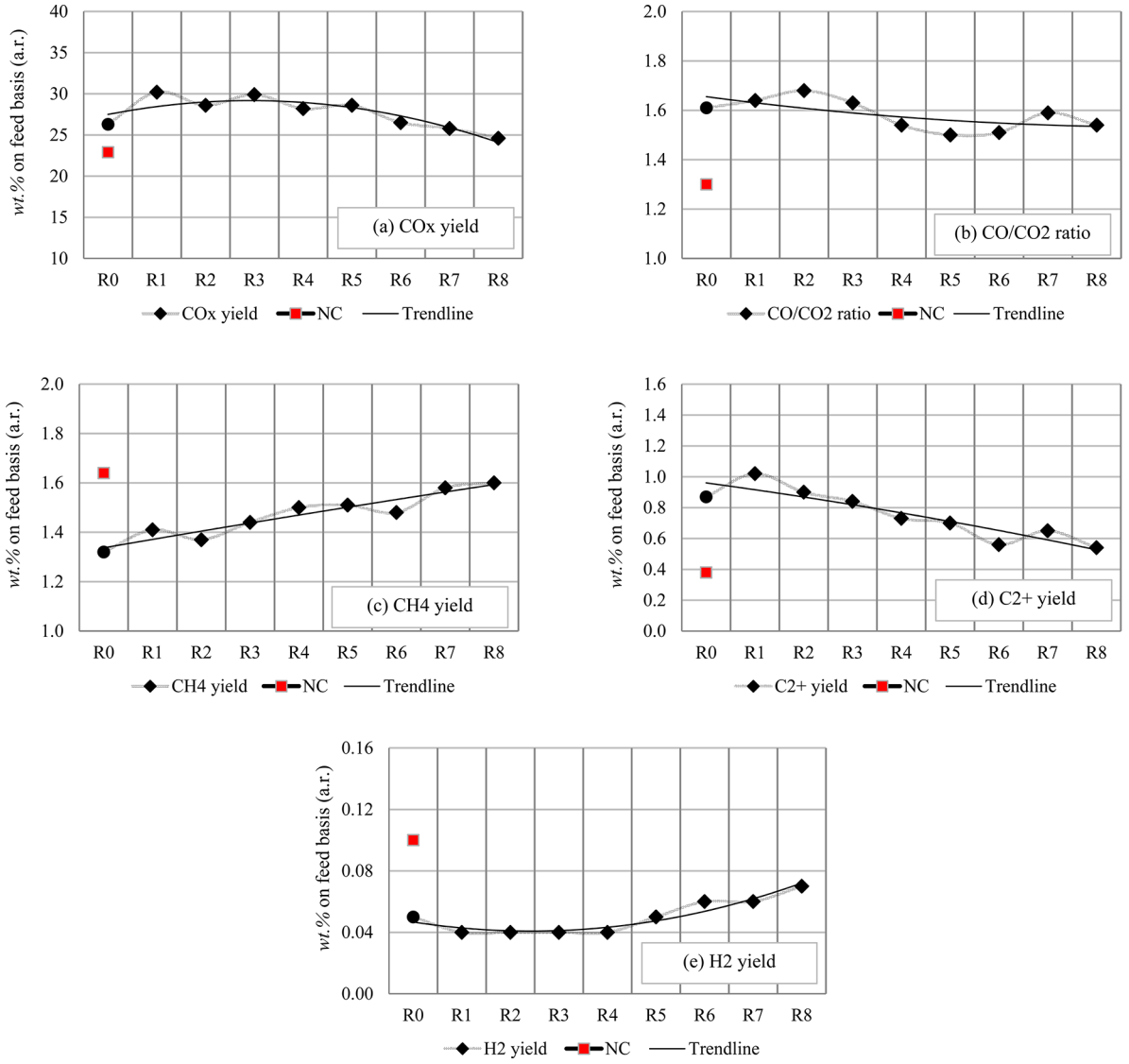

Figure 5. Changes in (a) CO_x yield (the sum of CO and CO_2), (b) CO/CO_2 ratio, (c) CH_4 yield, (d) C_{2+} yield (sum of C_2H_4, C_2H_6, C_3H_6, and C_3H_8), and (e) H_2 yield, obtained after successive reaction/regeneration cycles (R1 to R8, ◆). The results of noncatalytic (NC, red square) and catalytic fast pyrolysis with fresh catalyst (R0, ●) are included for comparison. Catalytic pyrolysis experiments of pine wood at 500 °C.

Figure 5e shows that on a weight basis H_2 seems to be a nondominant byproduct both in noncatalytic and catalytic pyrolysis. However, it is interesting to note that in the presence of the ZSM-5-based zeolite catalyst, the yield of H_2 is decreased by half (from 0.1 wt % to an average of 0.05 wt %). During the first four reaction/regeneration cycles, its value remained unchanged after which it slowly increased to the noncatalytic value. Apparently, in catalytic pyrolysis H_2 is consumed, which may contribute to the formation of hydrocarbons (dehydration reactions). While overlooking the results collected in Figure 5, it seems that the trends of the yields of individual noncondensable gas compounds are a good indicator of the catalyst deactivation, and it may be worthwhile to investigate such correlations in future investigations. Regarding the reduced hydrogen and methane yields observed for catalytic pyrolysis, this cannot be explained from a possible occurrence of the water gas shift reaction and/or methane reforming in the vapor phase. Methane is stable under the applied conditions, while the water gas shift reaction (in the presence of biomass minerals and the ZSM-5-based zeolite catalyst) would have resulted in an increase of hydrogen production while the carbon monoxide yield would have expected to decrease, which is not in line with the observations. Although the reasons for the reduced hydrogen and methane production remain unclear in this stage of research, it definitely is beneficial if all, or part, of the hydrogen lost from the noncondensable gases is preserved in the produced bio-oil.

3.5. Effect of Successive Catalyst Regeneration on the Bio-Oil Quality. Figure 6 shows the yield variations of the measured compounds using the GC × GC/MS-FID. The latter are classified according to their functional group and as a function of the number of catalyst regeneration cycles. The compounds were grouped as sugars, aldehydes, acids, furans, ketones, phenols, aromatics, and others (unclassified oxygenates). Table A.3 (in the Supporting Information) shows the details of the most prevalent individual compounds detected via GC × GC-TOF-MS analysis and quantified by GC × GC/MS-FID. For the quantification procedure, the reader is referred to the paper of Djokic et al.[36] It should be taken into account that the yields shown in Figure 6 and Table A.3 were normalized and expressed relative to the as-received feed basis.

dx.doi.org/10.1021/ef500636c | Energy Fuels 2014, 28, 4560−4572

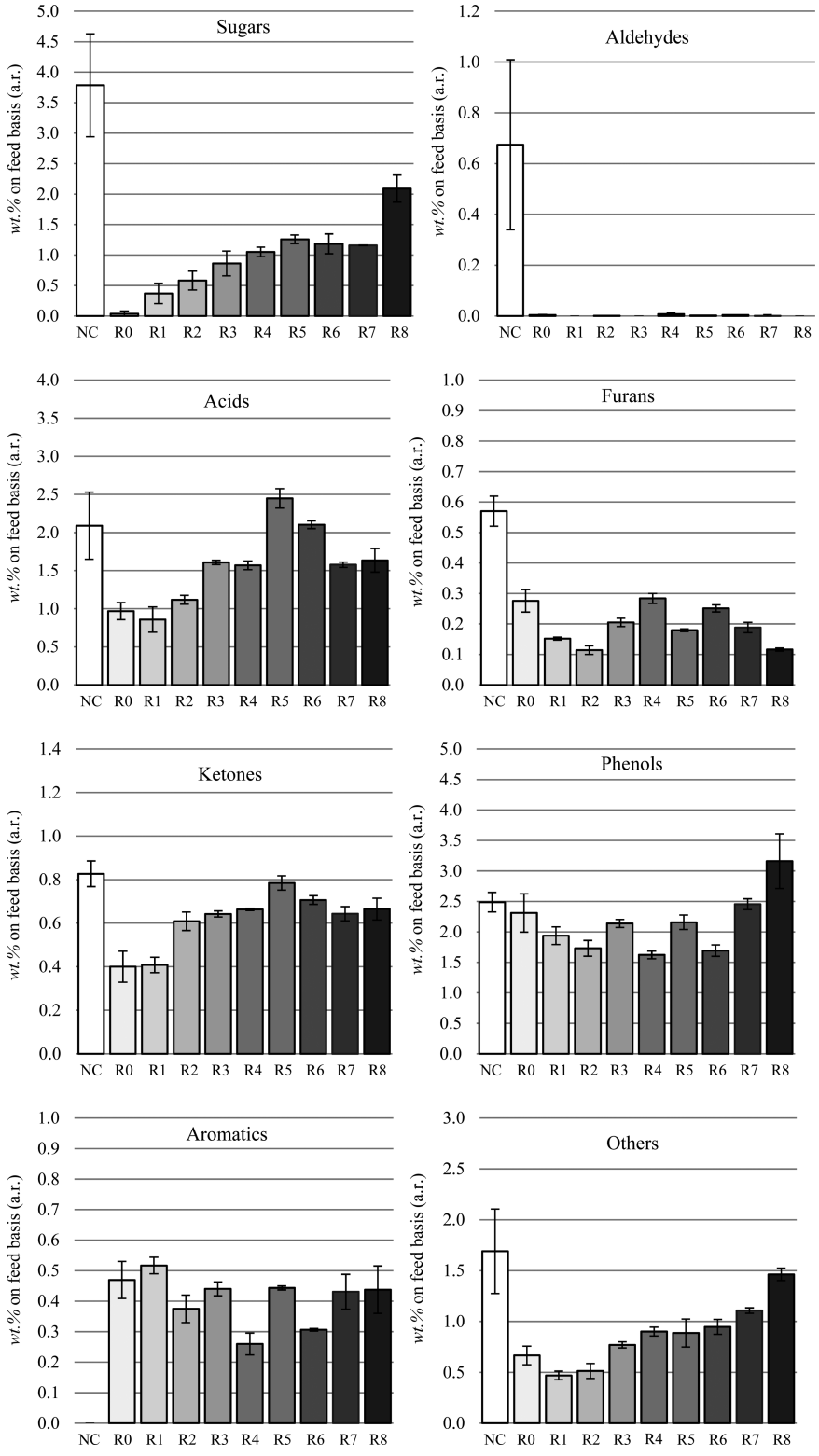

Figure 6. Results of pine wood experiments at 500 °C. Changes in bio-oil composition for successive reaction/regeneration cycles (R1 to R8). Bio-oil constituents were grouped according to their chemical functional groups (GC × GC/MS-FID detectable only). NC refers to noncatalytic pyrolysis as a reference case. R0 indicates catalytic fast pyrolysis with fresh catalyst. The yields are shown in wt % on feed basis (a.r.). Error bars represent standard deviations.

In bio-oil from noncatalytic pine wood pyrolysis, sugars constitute a high portion, and a mass fraction percentage of approximately 3.8 wt % was found by GC × GC/MS analysis. The most abundant sugar compound was levoglucosan with more than 3 wt % (Table A.3). In the presence of fresh catalyst, the amount of sugars was significantly reduced, and levoglucosan could not be observed anymore. This suggests that the amount of catalyst in the reactor bed is enough to retain its catalytic activity throughout the entire experimental run time. As the number of reaction/regeneration cycles increased, the quantity

dx.doi.org/10.1021/ef500636c | Energy Fuels 2014, 28, 4560−4572

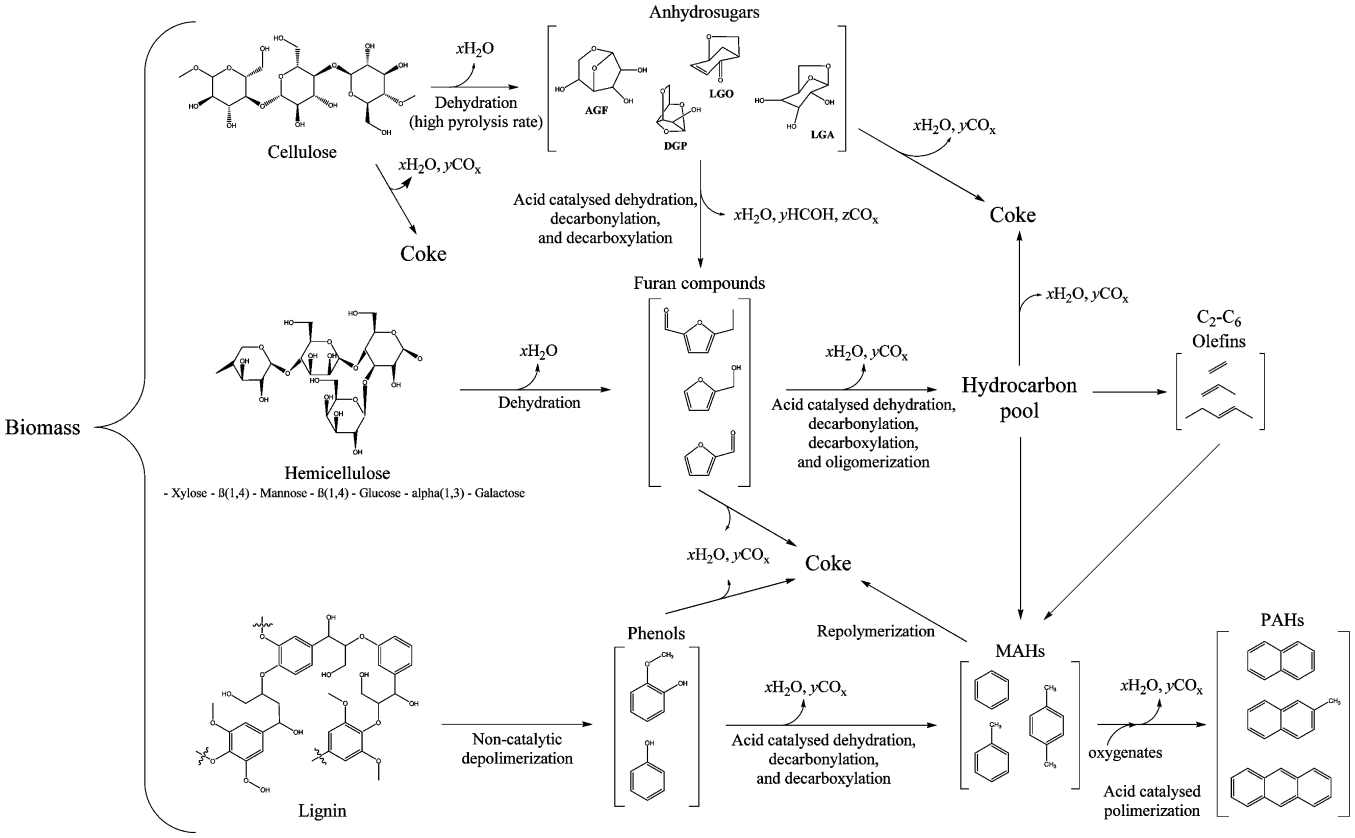

Figure 7. Reaction chemistry for the catalytic fast pyrolysis of biomass on solid acid catalyst. Scheme constructed from previously published suggestions.[11,32,47−49]

of sugars in bio-oil steadily rose again but without reaching the original level of the noncatalytic case. Although clearly present in the oil from noncatalytic pyrolysis, aldehydes (particularly hydroxyacetaldehyde) were completely undetectable when using fresh catalyst, as well as after any of the subsequent reaction/regeneration cycles. The quantity of detectable acids decreased during pyrolysis in the presence of a fresh catalyst (R0) by more than a factor 2. However, this effect largely disappeared again after repeated regeneration. Obviously acetic acid, the main detectable compound, was quite stable under the applied conditions. As concluded already in the previous subsection (increased CO/CO_2 ratio in the noncondensable gas), apparently the decarbonylation of particularly aldehyde functions is easier than the decarboxylation of acids.

Figure 7 shows the reaction chemistry for the catalytic fast pyrolysis of biomass over a solid acid catalyst. In pyrolysis, furans are produced from the dehydration of hemicellulose as well as by acid-catalyzed dehydration, decarbonylation, and decarboxylation of anhydrosugars. Produced furans are then converted to hydrocarbons and coke. Just like unsaturated compounds, furans produce large amounts of coke, which rapidly deactivates the zeolites.[50] The reason for the reduced levels of furans in Figure 6 was that most of the furans are converted to hydrocarbons to form monoaromatic hydrocarbons, olefins, and coke. The quantity of ketones decreased by half in catalytic pyrolysis with the fresh catalyst. After the second regeneration, however, ketones started to increase and stayed roughly constant along the subsequent regeneration cycles but always at a level below that of noncatalytic pyrolysis. While almost no aldehydes and sugars (and only minor amounts of ketones) were present in bio-oil obtained when using fresh catalyst, sugars and ketones increased notably after the catalyst had been regenerated. Although the literature suggests[51,52] that this would lead to an increased oxygen content and a reduced stability, Table 3 shows that the oxygen content of the produced bio-oil stays at a low level during many of the successive reaction/regeneration cycles.

Phenols are the result of a competition between their formation from lignin and their conversion to monoaromatic compounds (MAHs). They are supposed to originate from lignin depolymerization mainly. In the presence of acidic zeolites, phenols yield MAHs by (acid-catalyzed) dehydration, decarbonylation, and decarboxylation reactions. Besides, a considerable amount of phenols is lost due to coke formation (Figure 7). Hence, the performance of an acidic zeolite catalyst is directly related to the conversion rate of phenols to MAHs and coke. In Figure 6, a fluctuating trend around 2 wt % is observed until R6. In R7 and R8, the amount phenols increased remarkably up to 2.5 wt % and 3.2 wt %, respectively, the last value being even higher than for the noncatalytic pyrolysis case. All this shows that, as a consequence of increasing catalyst deactivation, the formation of phenols is gradually getting dominant over their conversion to monoaromatics.

In the noncatalytic bio-oil no aromatics were detected. In the presence of the catalyst, aromatics production was favored, but the amount was not consistently affected by the number of catalyst regenerations. Even in the last cycle (R8), similar quantities of aromatics were produced if compared to pyrolysis with the fresh catalyst. This shows that the catalyst remained active in terms of aromatics production. In the case of acidic zeolites such as ZSM-5, some of the heavy oligomers are cracked to light organics (mainly oxygenated), which may then

dx.doi.org/10.1021/ef500636c | Energy Fuels 2014, 28, 4560−4572

deposit on the catalyst surface and act as coke precursors.[53] Indeed, the major competing reaction to the formation of aromatics is the coke formation inside the zeolite particles, leading eventually to catalyst deactivation. In order to overcome this, fresh/regenerated catalyst would need to be fed continuously to the pyrolysis reactor, while spent catalyst is removed and regenerated in a separate vessel.[32]

Other compounds detectable in the bio-oil were the unclassified ones, of which 1-hydroxy-2-propanone was the most abundant one. The yield of these compounds dropped by almost 70% when going from the original noncatalytic case to the one of the fresh catalyst and then increased again to the noncatalytic level over all the subsequent reaction/regeneration cycles.

Although the effect varies for the different detectable compound groups, the general picture was that the catalyst activity is adversely influenced by the successive reaction/regeneration cycles. Starting from R0 (fresh catalyst), increasingly more acids, ketones, sugars, and unclassified oxygenates (others) were produced. Depending of course on what had happened to all the GC nondetectable compounds, this would cause the bio-oil to become ever more acidic, less stable, and less well deoxygenated when using a regenerated catalyst. It is obvious that repeated regeneration pushes the yields (always on biomass feed basis) of the various chemical compound groups back in the direction of the values of the noncatalytic bio-oil, with the exception of the phenols and aromatics. The latter are considered to be the compounds with the highest economic value and were still obtained in significant yields after eight regenerations. Clearly, the catalyst was not entirely deactivated and remains active in promoting the cracking of lignin and the subsequent formation of aromatics. Whether or not this would mean that the liquid product after eight reaction/regeneration cycles has, in every respect, a "better" quality than the original, noncatalytic bio-oil depends on its intended utilization and should be the subject of further research.

3.6. Effect of Successive Catalyst Regeneration on the Surface Area of the Catalyst. BET surface area analysis has been carried out for spent catalyst/sand mixtures and regenerated catalyst samples because the possible loss of surface area could be an indication of accumulated coke and tar inside the pores. The results are shown in Figure 8.

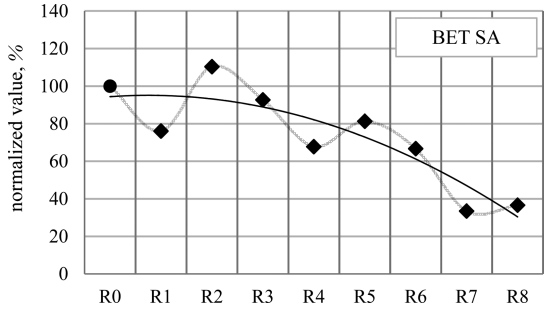

Figure 8. Normalized BET surface area values of ZSM-5-based catalyst for successive reaction/regeneration cycles (R1 to R8, ◆) resulting from experiments with pine wood at 500 °C. The data point for in situ catalytic fast pyrolysis with fresh catalyst (R0, ●) is included for a comparison.

The procedures and conditions applied during the regeneration play a vital role in the performance of the catalyst along the regeneration sequence. Although it was not possible to regain the surface area entirely, a fair retention of surface area was obtained in the first three to five regenerations. However, during the last few cycles, the surface area appeared to be reduced drastically. With some fluctuations along the regeneration sequence (a declining trend), the surface area recovery decreased to 37% in R8. Hence, it can be concluded that successive catalyst regeneration causes a significant loss of the catalyst surface area, which causes partial deactivation. Although the catalyst seems regenerable to a certain extent, and the regeneration procedure was successful for at least a number of cycles, eventually the BET surface area collapses due to an accumulative and permanent coke/ash deposition on the catalyst.

4. CONCLUSIONS

Noncatalytic and in situ catalytic pyrolysis of pine wood at 500 °C have been examined in a mechanically stirred sand bed reactor to observe the effects of both catalysis and repeated catalyst regeneration, on the pyrolysis products yields and quality. For catalytic pyrolysis, fresh and regenerated ZSM-5-based catalyst particles were mixed with the sand in ratios of about 1:14. After each catalytic pyrolysis experiment, the catalyst was regenerated in air by a programmed temperature procedure reaching up to 600 °C. In total, eight reaction/regeneration cycles were carried out to derive the change in catalyst activity (deactivation) over the increasing number of cycles. The accuracy of the measurements was shown to be high enough for determining clear trends in the yields of the gaseous, liquid, and solid products.

Regarding the yields, it was observed that the values for the produced water, carbonaceous solids, and noncondensable gases in catalytic pyrolysis are all well above (20−30% on average) the values for the noncatalytic case. However, the organics liquid yield is drastically reduced, roughly by a factor two. While looking at the yield trends as a function of the number of reaction/regeneration cycles, they pass through a flat minimum (organics liquid) or maximum (water and noncondensable gases), however, with the exception of the carbonaceous solids whose yield shows a straight, slightly increasing trend. Apparently the catalyst is more active during the first two cycles but clearly loses its activity in the last few cycles. Then, the catalyst regeneration becomes much less efficient, and the yields tend to return to the values of the noncatalytic pyrolysis.

All this was confirmed by the observed yields of the noncondensable gases over the successive reaction/regeneration cycles. Methane and hydrogen productions were clearly suppressed in catalytic pyrolysis, while the formation of carbon monoxide and small hydrocarbons (C_{2+}) was promoted. On a mole basis, ca. 90% of the noncondensable gas consists of carbon monoxide and carbon dioxide. But the course of the methane yield in particular, as a function of the number of reaction/regeneration cycles, seems to be a good indicator of the decreasing catalyst activity (straight increasing trend line, back to the noncatalytic value).

More indications of the catalyst activity were found in the results of the bio-oil GC/MS analysis. The most pronounced effect of catalysis is in the disappearance of sugars and aldehydes. For most of the detectable compounds (sugars, acids, ketones, unclassified oxygenates), values decrease initially in the first few reaction/regeneration cycles but then climb again to the noncatalytic values. Aromatics (not detected in the

case of noncatalytic pyrolysis!) are being produced over the entire series of reaction/regeneration cycles, showing that the catalyst maintains its activity with respect to these, possibly valuable compounds.

The catalyst activity was further explored by BET surface analysis which indeed revealed a decrease in the surface area over the last four reaction/regeneration cycles. The final fraction left is just 37% of the original BET surface area. In agreement with this reduced catalyst activity potential seems to be the measured coke-on-catalyst, which decreases from 6 to 2 wt % of the biomass feed.

It finally appeared that the energy lost in the noncondensable gases and carbonaceous solids (byproducts) is significant. While in the noncatalytic pyrolysis case 58% of the energy was retained in the bio-oil, this was reduced to around 45−48% in the worst cases of catalytic pyrolysis, viz., after 1−4 catalyst regenerations.

Although multiple, full regeneration of the ZSM-5-based catalyst appeared impossible, its activity with respect to the production of aromatics and phenols was largely maintained over a series of eight reaction/regeneration cycles. Although beneficial effects of catalysis were observed, obviously the conditions for catalytic pyrolysis were suboptimal. New catalyst formulations, vapor phase treatment instead of in situ catalysis, improved catalyst regeneration procedures, application of other temperatures, and optimization of space velocities are all possible strategies to further improve the result of catalytic fast pyrolysis.

■ ASSOCIATED CONTENT

Ⓢ Supporting Information

This material is available free of charge via the Internet at http://pubs.acs.org.

■ AUTHOR INFORMATION

Corresponding Author

*Telephone: +32 (0) 264 6190; fax: +32 (0) 264 6235; e-mail: guray.yildiz@ugent.be, guryildiz@gmail.com.

Notes

The authors declare no competing financial interest.

■ ACKNOWLEDGMENTS

B. Knaken and J. F. H. Agterhorst of Sustainable Process Technology (SPT) group of University of Twente (Enschede, The Netherlands) are acknowledged for the construction of the experimental unit. Robbie Venderbosch is acknowledged for his efforts during the reviewing process. The research leading to these results has received funding from Ghent University Special Research Fund (BOF) and from the European Research Council under the European Union's Seventh Framework Programme FP7/2007-2013/ERC Grant Agreement No. 290793.

■ NOMENCLATURE

Roman Variables

Y = yield, wt % on feed (a.r.)
m = mass, kg
T = temperature, °C
wt % = weight percentage, g/g
vol % = volume percentage
t_{run} = experimental run time, min
Φ_{pine} = flow rate of pine wood, g/h
Φ_{N2} = inert gas flow rate, L/h
U = superficial gas velocity, m/s
U_{mf} = minimum fluidization velocity, m/s
τ = residence time, s
WHSV = weight hourly space velocity, h^{-1}
d.b. = on a dry feedstock basis
a.r. = as received
s = seconds
L.O.I. = loss of ignition (burning the char and coke with air)

Subscripts

pine = biomass feedstock used
bed material = sand or sand-catalyst mixture introduced to the reactor
vapors = generated pyrolysis vapors
bio-oil = liquid product (including generated water)
ESP,out = electrostatic precipitator subsequent to the experiment
ESP,in = electrostatic precipitator prior to the experiment
gc,out = glass spiral condenser subsequent to the experiment
gc,in = glass spiral condenser prior to the experiment
cf,out = cotton filter subsequent to the experiment
cf,in = cotton filter prior to the experiment
fs = filtrate solids
solids,i = carbonaceous solids (sum of char, heterogeneous coke, and system deposits), before L.O.I.
solids,f = carbonaceous solids (sum of char, heterogeneous coke, and system deposits), after L.O.I.

■ REFERENCES

(1) Hu, C.; Yang, Y.; Luo, J.; Pan, P.; Tong, D.; Li, G. *Front. Chem. Sci. Eng.* **2011**, *5*, 188−193.
(2) Goyal, H.; Seal, D.; Saxena, R. *Renewable Sustainable Energy Rev.* **2008**, *12*, 504−517.
(3) Venderbosch, R.; Prins, W. *Biofuels, Bioprod. Biorrefin.* **2010**, *4*, 178−208.
(4) Meier, D.; van de Beld, B.; Bridgwater, A. V.; Elliott, D. C.; Oasmaa, A.; Preto, F. *Renewable Sustainable Energy Rev.* **2013**, *20*, 619−641.
(5) Bridgwater, T. *J. Sci. Food Agric.* **2006**, *86*, 1755−1768.
(6) Lappas, A.; Samolada, M.; Iatridis, D.; Voutetakis, S.; Vasalos, I. *Fuel* **2002**, *81*, 2087−2095.
(7) Czernik, S.; Bridgwater, A. V. *Energy Fuels* **2004**, *18*, 590−598.
(8) Bridgwater, A. V. *Biomass Bioenerg.* **2012**, *38*, 68−94.
(9) Jackson, M. A.; Compton, D. L.; Boateng, A. A. *J. Anal. Appl. Pyrolysis* **2009**, *85*, 226−230.
(10) Dickerson, T.; Soria, J. *Energies* **2013**, *6*, 514−538.
(11) Mochizuki, T.; Chen, S.-Y.; Toba, M.; Yoshimura, Y. *Appl. Catal., A* **2013**, *456*, 174−181.
(12) Pattiya, A.; Titiloye, J. O.; Bridgwater, A. *J. Anal. Appl. Pyrolysis* **2008**, *81*, 72−79.
(13) Zhang, H.; Xiao, R.; Jin, B.; Shen, D.; Chen, R.; Xiao, G. *Bioresour. Technol.* **2013**, *137*, 82−87.
(14) Morris, M. A. *Handbook of Biofuels Production*; Woodhead Publishing Limited: Sawston, Cambridge, 2011; pp 349−389.
(15) Pattiya, A.; Titiloye, J. O.; Bridgwater, A. *Fuel* **2010**, *89*, 244−253.
(16) Jae, J.; Tompsett, G. A.; Foster, A. J.; Hammond, K. D.; Auerbach, S. M.; Lobo, R. F.; Huber, G. *J. Catal.* **2011**, *279*, 257−268.
(17) Carlson, T. R.; Vispute, T. P.; Huber, G. W. *ChemSusChem* **2008**, *1*, 397−400.
(18) Park, H. J.; Jeon, J.-K.; Suh, D. J.; Suh, Y.-W.; Heo, H. S.; Park, Y.-K. *Catal. Surv. Asia* **2011**, *15*, 161−180.
(19) Zhang, H.; Cheng, Y.-T.; Vispute, T. P.; Xiao, R.; Huber, G. W. *Energy Environ. Sci.* **2011**, *4*, 2297−2307.
(20) Qiang, L.; Zhi, L. W.; Dong, Z.; Feng, Z. X. *J. Anal. Appl. Pyrolysis* **2009**, *84*, 131−138.

(21) Bartholomew, C. H. *Appl. Catal., A* **2001**, *212*, 17−60.
(22) Guisnet, M.; Riberio, F. R. *Deactivation and Regeneration of Solid Catalysts*; Imperial College Press: UK, 2011; pp 3−18.
(23) Guisnet, M.; Magnoux, P. *Catal. Today* **1997**, *36*, 477−483.
(24) Cerqueira, H.; Caeiro, G.; Costa, L.; Ribeiro, F. R. *J. Mol. Catal. A: Chem.* **2008**, *292*, 1−13.
(25) Marcilla, A.; Beltran, M.; Hernandez, F.; Navarro, R. *Appl. Catal., A* **2004**, *278*, 37−43.
(26) Cerqueira, H. S.; Ayrault, P.; Datka, J.; Guisnet, M. *Microporous Mesoporous Mater.* **2000**, *38*, 197−205.
(27) Triantafillidis, C. S.; Vlessidis, A. G.; Nalbandian, L.; Evmiridis, N. P. *Microporous Mesoporous Mater.* **2001**, *47*, 369−388.
(28) Aho, A.; Kumar, N.; Lashkul, A.; Eranen, K.; Ziolek, M.; Decyk, P.; Salmi, T.; Holmbom, B.; Hupa, M.; Murzin, D. Y. *Fuel* **2010**, *89*, 1992−2000.
(29) Aho, A.; Kumar, N.; Eranen, K.; Salmi, T.; Hupa, M.; Murzin, D. Y. *Fuel* **2008**, *87*, 2493−2501.
(30) Aho, A.; Kumar, N.; Eranen, K.; Salmi, T.; Hupa, M.; Murzin, D. Y. *Process Saf. Environ.* **2007**, *85*, 473−480.
(31) Williams, P. T.; Horne, P. A. *Fuel* **1995**, *74*, 1839−1851.
(32) Carlson, T. R.; Cheng, Y. T.; Jae, J.; Huber, G. W. *Energy Environ. Sci.* **2011**, *4*, 145−161.
(33) Paasikallio, V.; Lindfors, C.; Lehto, J.; Oasmaa, A.; Reinikainen, M. *Top. Catal.* **2013**, *56*, 800−812.
(34) https://www.ecn.nl/phyllis/defs.asp.
(35) Yildiz, G.; Pronk, M.; Djokic, M.; van Geem, K. M.; Ronsse, F.; van Duren, R.; Prins, W. *J. Anal. Appl. Pyrolysis* **2013**, *103*, 343−351.
(36) Djokic, M. R.; Dijkmans, T.; Yildiz, G.; Prins, W.; van Geem, K. M. *J. Chromatogr., A* **2012**, *1257*, 131−140.
(37) Van Geem, K. M.; Pyl, S. P.; Reyniers, M.-F.; Vercammen, J.; Beens, J.; Marin, G. B. *J. Chromatogr., A* **2010**, *1217* (43), 6623−6633.
(38) Pyl, S. P.; Schietekat, C. M.; Van Geem, K. M.; Reyniers, M.-F.; Vercammen, J.; Beens, J.; Marin, G. B. *J. Chromatogr., A* **2011**, *1218* (21), 3217−3223.
(39) Schofield, K. *Prog. Energy Combust.* **2008**, *34* (3), 330−350.
(40) Zabeti, M.; Nguyen, T.; Lefferts, L.; Heeres, H.; Seshan, K. *Bioresour. Technol.* **2012**, *118*, 374−381.
(41) Butler, E.; Devlin, G.; Meier, D.; McDonnell, K. *Renewable Sustainable Energy Rev.* **2011**, *15*, 4171−4186.
(42) Bridgwater, A. V. *J. Anal. Appl. Pyrolysis* **1999**, *51*, 3−22.
(43) Bridgwater, A.; Meier, D.; Radlein, D. *Org. Geochem.* **1999**, *30*, 1479−1493.
(44) Foster, A. J.; Jae, J.; Cheng, Y.-T.; Huber, G. W.; Lobo, R. F. *Appl. Catal. A* **2012**, *423*−*424*, 154−161.
(45) Carlson, T.; Tompsett, G.; Conner, W.; Huber, G. W. *Top. Catal.* **2009**, *52*, 241−252.
(46) Agblevor, F. A.; Beis, S.; Mante, O.; Abdoulmoumine, N. *Ind. Eng. Chem. Res.* **2010**, *49*, 3533−3538.
(47) Mullen, C. A.; Boateng, A. A. *Fuel Process. Technol.* **2010**, *91*, 1446−1458.
(48) Tan, S.; Zhang, Z.; Sun, J.; Wang, Q. *Chin. J. Catal.* **2013**, *34*, 641−650.
(49) Ma, Z.; Troussard, E.; van Bokhoven, J. A. *Appl. Catal., A* **2012**, *423*−*424*, 130−136.
(50) Zhang, H.; Cheng, Y.-T.; Vispute, T. P.; Xiao, R.; Huber, G. W. *Energy Environ. Sci.* **2011**, *4*, 2297−2307.
(51) Oasmaa, A.; Kuoppala, E. *Energy Fuel.* **2003**, *17*, 1075−1084.
(52) Nokkosmaki, M.; Kuoppala, E.; Leppamaki, E.; Krause, A. *J. Anal. Appl. Pyrolysis* **2000**, *55*, 119−131.
(53) Vitolo, S.; Bresci, B.; Seggiani, M.; Gallo, M. *Fuel* **2001**, *80*, 17−26.